Journal of Cellular Physiology

TRPC1 Regulates Calcium-Activated Chloride Channels in Salivary Gland Cells

YUYANG SUN,[1] LUTZ BIRNBAUMER,[2] AND BRIJ B. SINGH[1]*

[1]Department of Basic Sciences, School of Medicine Health Sciences, University of North Dakota, Grand Forks, North Dakota

[2]Laboratory of Signal Transduction, NIHES, NIH, Research Triangle Park, North Carolina

Calcium-activated chloride channel (CaCC) plays an important role in modulating epithelial secretion. It has been suggested that in salivary tissues, sustained fluid secretion is dependent on Ca^{2+} influx that activates ion channels such as CaCC to initiate Cl^- efflux. However direct evidence as well as the molecular identity of the Ca^{2+} channel responsible for activating CaCC in salivary tissues is not yet identified. Here we provide evidence that in human salivary cells, an outward rectifying Cl^- current was activated by increasing $[Ca^{2+}]_i$, which was inhibited by the addition of pharmacological agents niflumic acid (NFA), an antagonist of CaCC, or T16Ainh-A01, a specific TMEM16a inhibitor. Addition of thapsigargin (Tg), that induces store-depletion and activates TRPC1-mediated Ca^{2+} entry, potentiated the Cl^- current, which was inhibited by the addition of a non-specific TRPC channel blocker SKF96365 or removal of external Ca^{2+}. Stimulation with Tg also increased plasma membrane expression of TMEM16a protein, which was also dependent on Ca^{2+} entry. Importantly, in salivary cells, TRPC1 silencing, but not that of TRPC3, inhibited CaCC especially upon store depletion. Moreover, primary acinar cells isolated from submandibular gland also showed outward rectifying Cl^- currents upon increasing $[Ca^{2+}]_i$. These Cl^- currents were again potentiated with the addition of Tg, but inhibited in the presence of T16Ainh-A01. Finally, acinar cells isolated from the submandibular glands of TRPC1 knockout mice showed significant inhibition of the outward Cl^- currents without decreasing TMEM16a expression. Together the data suggests that Ca^{2+} entry via the TRPC1 channels is essential for the activation of CaCC.

J. Cell. Physiol. 230: 2848–2856, 2015. *Journal of Cellular Physiology* Published by Wiley Periodicals, Inc.

Calcium-activated chloride channel (CaCC) is fundamental to many cellular functions such as regulation of membrane potential in excitable cells, smooth muscle contraction, and fluid secretion by exocrine cells (Ferrera et al., 2010; Ferrera et al., 2011; Huang et al., 2012). Non-excitable cells, such as airway epithelial cells, transport Cl^- to control the amount of airway surface, which is important for the hydration and protection of airway epithelial cells against infections. Cl^- efflux through the apical membrane is also essential for the vectorial transport of electrolytes and water in secretory epithelial cells present in the kidney, airways, intestine, pancreas, and salivary gland. Acinar cells from lachrymal, parotid, submandibular, and sublingual glands, as well as in the pancreas, also express CaCCs with similar properties, but their mode of regulation is not clear. For fluid secretion, CaCC is suggested to be the major apical Cl^- efflux channel required by exocrine glands (Frizzell and Hanrahan, 2012), which drives the movement of Na^+ through the parallel pathway, thereby resulting in fluid secretion. However, characterization of the Cl^- efflux channel and understanding of its regulation mechanism(s) in salivary cells is not well established.

The recent discovery of the transmembrane proteins of unknown function 16 (TMEM16a, also termed ANO) has been identified as CaCC channels and TMEM16a channels have been shown to generate CaCC currents in vitro that are dependent on physiological intracellular Ca^{2+} concentrations (Caputo et al., 2008; Schroeder et al., 2008; Ferrera et al., 2010; Thomas-Gatewood et al., 2011). TMEM16a channels are widely expressed in epithelial cells, including salivary glands and disruption of the TMEM16a gene in mice eliminates Ca^{2+}-dependent Cl^- secretion in several epithelial tissues including salivary glands (Yang et al., 2008; Huang et al., 2009; Ousingsawat et al., 2009; Romanenko et al., 2010; Catalan et al., 2015). Cl^- secretion via CaCCs is activated by the rise of intracellular Ca^{2+} levels, but the source and the ion channels involved in increasing intracellular Ca^{2+} levels are not known. Members of the transient receptor potential (TRP) superfamily are present from nematodes to mammals and function as ion channels that have a fundamental role in cell physiology. TRP channels have been shown to exhibit high Ca^{2+} permeability, which could regulate TMEM16a, thereby modulating numerous physiological functions. Importantly, TRPV4 has been reported to physically interact with TMEM16a in choroid plexus epithelial cells (Takayama et al., 2014) and TRPC2 has been shown to functionally couple with TMEM16a in rat thyroid cells

Abbreviations: sCaCCs, calcium-activated chloride channels; NFA, niflumic acid; Tg, thapsigargin; CCh, carbachol; TRP, transient receptor potential; SOCE, store operated calcium entry; SOCC, store operated calcium channels; SMG, submandibular gland.

Conflict of interest: The authors declared that they have no competing interests.

Contract grant sponsor: National Institutes of Health;
Contract grant number: DE017102.
Contract grant sponsor: Intramural Research Program of the NIH;
Contract grant number: Z01-ES-101684.

*Correspondence to: Brij B. Singh, Department of Basic Sciences, School of Medicine and Health Sciences, University of North Dakota, Grand Forks, ND 58201.
E-mail: brij.singh@med.und.edu

Manuscript Received: 26 March 2015
Manuscript Accepted: 14 April 2015

Accepted manuscript online in Wiley Online Library (wileyonlinelibrary.com): 21 April 2015.
DOI: 10.1002/jcp.25017

(Viitanen et al., 2013). However, the activation of TMEM16a channels specifically via TRPC1 channel in salivary gland cells is not known.

The canonical transient receptor potential cation channel isoform 1 (TRPC1) is primarily activated by store-depletion and has been suggested as a component of store operated Ca^{2+} entry channels (SOCC) (Liu et al., 2003; Ong et al., 2007). TRPC1 channels have been identified in salivary gland cells (Liu et al., 2003, 2007; Pani et al., 2013). Importantly in human salivary gland (HSG) cells, knock-down of TRPC1 suppressed store-operated Ca^{2+} influx without affecting Ca^{2+} release from the internal stores, suggesting that Ca^{2+} influx via TRPC1 contributes to the increase in $[Ca^{2+}]_i$. Our pervious study has also shown that TRPC1 was important for fluid secretion (Liu et al., 2007). Agonist- and thapsigargin-induced Ca^{2+} entry was significantly reduced in salivary gland acinar cells isolated from TRPC1 knockout mice. Furthermore, neurotransmitter-regulated salivary gland fluid secretion in TRPC1-deficient mice was severely decreased, suggesting that TRPC1-mediated Ca^{2+} entry is required for neurotransmitter-induced saliva secretion. However, the relationship between TRPC1 and TMEM16a and the mechanism(s) as to how TRPC1 modulates saliva secretion remains unknown. The data presented here indicate that TMEM16a functions as an endogenous CaCC channel in salivary gland cells. Interestingly, the activity of TMEM16a channel was regulated by Ca^{2+} entry upon store-depletion and inhibition of TRPC1-mediated Ca^{2+} entry and decreased Cl^- currents. Finally, acinar cells from TRPC1 knockout mice showed a significant reduction in TMEM16a currents, indicating that TRPC1 is critical for TMEM16a activity in salivary gland cells.

Materials and Methods

Cell culture reagents and transfection

HSG cells were cultured/maintained at 37°C with 95% humidified air and 5% CO_2 as described before (Liu et al., 2000). Culture medium was changed twice weekly and cells were maintained in complete media, until reaching 90% confluence. Transient transfection HSG cells (1.5×10^5 cells/ml) were transfected with TRPC1 siRNA or TRPC3 siRNA (Ambion, Austin, TX) or scrambled control siRNA (Ambion negative control siRNA) using Lipofectamine 2000 (Ambion) in Opti-MEM medium as per supplier's instructions (Invitrogen, Carlsbad, CA) and assayed after 48 h. Antibodies used in this study are described in the figures. All other reagents used were obtained from Sigma (St. Louis, MO) unless mentioned otherwise.

Animals and acinar cell isolation

Six-to-eight weeks old TRPC1$^{-/-}$ and wild type mice were used for these experiments. The TRPC1$^{-/-}$ mice were generated as previously described (Liu et al., 2007). All animals were housed in a temperature controlled room under a 12/12 h light/dark cycle with ad libitum access to food and water. All animal experiments were carried out as per the institutional guidelines for the use and care of animals. Cells were prepared from the mouse submandibular glands (SMG), by removing the submandibular glands, which was cleaned, minced, and digested in standard extracellular solution buffer containing 0.1% bovine serum albumin and collagenase-II (2.5 mg/8 ml) for 15–20 min at 37°C. Cells were washed twice with the external solution and re-suspended in 5 ml of standard extracellular solution buffer prior to experimental use.

Chloride measurements

Cells were incubated with 10 mM SPQ (Molecular Probes, Eugene, OR) for 45 min. For fluorescence measurements, cells were monitored with a CCD camera-based imaging system (Compix Inc., Cranbery, PA) mounted on an Olympus XL70 inverted microscope equipped with an Olympus 40 × (1.3 NA) objective. Images were acquired by excitation at 344 nM and emission was monitored at 510 nm with an Orca Imaging camera (Hamamatsu, Japan). The images of multiple cells collected were processed using the C imaging, PCI software (Compix). Data are presented as F_0/F units essentially as described previously (Lee and Foskett, 2010; Romanenko et al., 2010), with a ratio generated by dividing the average fluorescence during the 1 min time period obtained at rest just prior to stimulation (F_0) by the fluorescence values (F) obtained throughout the experiment.

Cell surface biotinylation

Cells were stimulated with thapsigargin (2 μM) with and without calcium for 5 min and were incubated for 20 min with 0.5 mg/ml Sulfo-NHS-Biotin (Pierce) in 1XPBS (pH 8.0) on ice with gentle rocking. Following biotin labeling cells were washed with 1XPBS with and without Ca^{2+} (pH 7.4) and 100 mM glycine. Cells were solubilized with 1X RIPA buffer and biotinylated proteins were pulled down with NeutrAvidin-linked beads (Pierce). Bound fraction was washed and released with 1X SDS–PAGE followed by Western blotting. Band intensities of surface proteins were obtained using Quantity one 4.6.5 1D-analysis software (BioRad, Hercules, CA).

Electrophysiology

For patch clamp experiments, coverslips with cells were transferred to the recording chamber and perfused with an external Ringer's solution of the following composition (mM): Tetraethylammonium(TEA)-Cl, 145; $MgCl_2$, 1; $CaCl_2$, 2; Hepes, 10; Glucose, 10; pH 7.3 (Tris). Whole cell currents were recorded using an Axopatch 200B (Axon Instruments, Inc., Sunnyvale, CA). The patch pipette had resistances between 3–5 MΩ after filling with the standard intracellular solution that contained the following (mM): TEA-Cl, 145; MgATP, 3; Hepes, 10; EGTA, 5; pH 7.2 (Tris). Total $CaCl_2$ were adjusted to 300 nM (high) or 30 nM (low) free Ca^{2+}, respectively. Free Ca^{2+} was calculated using WebmaxC Standard (http://www.stanford.edu/~cpatton/webmaxcS.htm). The stimulation protocol to generate current–voltage relationships consisted in 2 sec long voltage steps from − 100 to + 100 mV in 20 mV increments starting from a holding potential of − 60 mV. For CFTR currents recording, intracellular solution contained the following (mM): CsCl, 140; TEA-Cl, 10; MgATP, 1; Hepes, 10; EGTA, 0.1; pH 7.2 (CsOH). Currents were recorded at 2 kHz and digitized at 5–8 kHz. pClamp 10.1 software was used for data acquisition and analysis. Basal leak was subtracted from the final currents and average currents are shown. All experiments were carried out under room temperature.

Membrane preparations and Western blot analyses

Cells were harvested and stored at −80°C. Crude lysates were prepared from HSG cells and animal tissue as described previously (Liu et al., 2010; Pani et al., 2013). Protein concentrations were determined using Bradford reagent (BioRad) and 25 ug of lysates were resolved on NuPAGE 4-12% Bis-Tris gel (Invitrogen) followed by Western blotting as described (Pani et al., 2013; Sun et al., 2014).

Statistical analysis

Data analysis was performed using Origin 9.0 (OriginLab, Northampton, MA). Statistical comparisons were made using Student's *t*-test. Experimental values are expressed as means ± S.D or means ± S.E. Differences in the mean values were considered to be significant at $P < 0.05$.

Results

Chloride currents are present in HSG cells

Ca^{2+}-activated Cl^- channels (CaCC) are modulated by an increase in intracellular Ca^{2+} levels ($[Ca^{2+}]_i$), which shows both time and voltage dependent activation kinetics essential for modulating exocrine functions (Hartzell et al., 2005; Huang et al., 2012). Although CaCC has been shown to be regulated by $[Ca^{2+}]_i$, the molecular identity of the Ca^{2+}-influx channel is not known. We show here that human salivary gland (HSG) cells exhibit an outward rectifying Cl^- current that was prompted using a voltage step protocol in conditions where free $[Ca^{2+}]_i$ is increased (Fig. 1A,E). The properties of the Cl^- current were consistent with previous recordings observed in different cells that are linked with CaCC (Ferrera et al., 2010; Huang et al., 2012). Addition of niflumic acid (NFA, 100 μM), an antagonist of CaCC, dramatically inhibited the outward Cl^- current (Fig. 1B,E,F). To directly test the role of intracellular Ca^{2+} on the activation of Cl^- currents, the free $[Ca^{2+}]_i$ was decreased to near 0 nM, which completely blocked the Cl^- currents in HSG cells (Fig. 1C,E,F). More importantly, application of T16Ainh-A01 (10 μM), a specific TMEM16a inhibitor (Davis et al., 2013), also blocked the outward Cl^- currents (Fig. 1D,E,F), indicating that the CaCC channels in HSG cells are indeed mediated by TMEM16a. To further establish the role of $[Ca^{2+}]_i$ in the activation of CaCC we gradually increased the $[Ca^{2+}]_i$ concentration, which showed a sigmoid relationship with the maximum activation of the Cl^- currents observed at 1 μM $[Ca^{2+}]_i$ (Fig. 1G). Besides TMEM16a, cystic fibrosis transmembrane conductance regulator (CFTR) channels have also been shown to regulate Cl^- currents in secretory cells and loss of CFTR has been shown to disrupt secreted fluid volume and composition. Thus, we also evaluated CFTR currents in HSG cells where cAMP-induced activation of CFTR currents was observed in HSG cells, which was inhibited by the addition of a specific CFTR inhibitor ($CFTR_{inh}$-172) (Supplemental Figure S1 A–D). However, addition of $CFTR_{inh}$-172 failed to inhibit CaCC currents in HSG cells (Supplemental Figure S1 E,F). Together, these results suggest that the outwardly rectifying Cl^- currents in HSG cells is mediated by TMEM16a, which is likely to be activated by an increase in $[Ca^{2+}]_i$.

Chloride currents are regulated by store-operated calcium entry in HSG cells

Data presented in Figure 1 indicates $[Ca^{2+}]_i$ is essential for the activation of CaCC in HSG cells, which is mediated via TMEM16a; however, the source of $[Ca^{2+}]_i$ is not known. Thus, we used two-different mechanisms including addition of thapsigargin (Tg) (a SERCA pump blocker that causes release of Ca^{2+} from the ER stores) or agonist (CCh, carbachol) mediated depletion of ER stores to activate store-operated Ca^{2+} entry. Importantly, in the absence of external Ca^{2+} ($[Ca^{2+}]_{out}$), Tg (2 μM) failed to activate the Cl^- currents

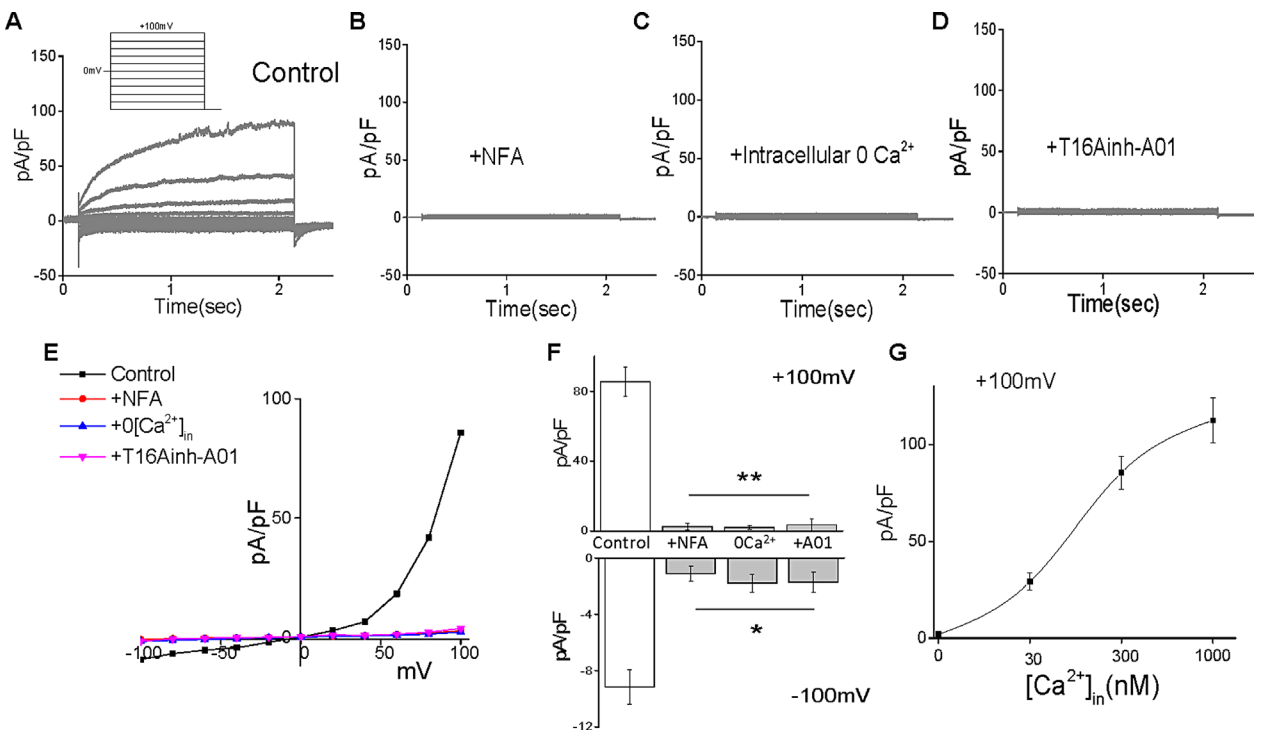

Fig. 1. Increase in intracellular Ca^{2+} develop an outward Cl^- current that was dependent on TMEM16a in HSG cells: (A) Representative trace from HSG cells showing an outward Cl^- current that was prompted using a voltage step protocol in conditions of 300 nM of free intracellular Ca^{2+}. (B), Bath application of 100 μM niflumic acid (NFA) inhibited CaCC current. The current with a free intracellular Ca^{2+} 0 nM is shown in (C). (D), Bath application of 10 μM T16Ainh-A01 blocked CaCC current activated by 300 nM of free intracellular Ca^{2+}. Average IV curves (developed from maximum currents) under these conditions are shown in (E). (F) Average (8–10 recordings) current density under these conditions is shown. *indicates values (representing mean ± SE) that are significantly different from control ($^*P < 0.05$, $^{**}P < 0.01$). (G) Dependence of the CaCC currents on internal $[Ca^{2+}]$ was evaluated using intracellular Ca^{2+} concentrations ranging from near 0 to 1,000 nM.

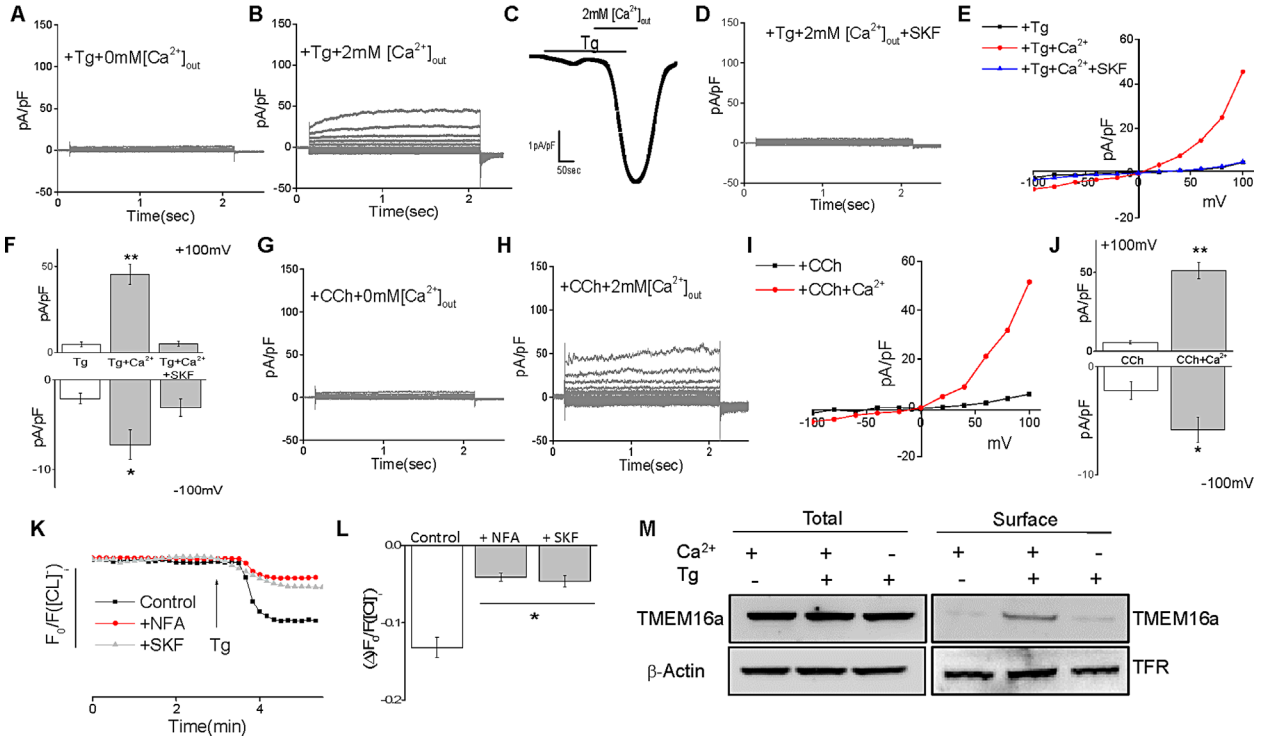

Fig. 2. CaCC currents are regulated by store-operated calcium entry in HSG cells: (A) (B), Representative traces showing CaCC currents (with a free intracellular Ca^{2+} 0 nM) under conditions of bath application 2 μM Tg with or without 2 mM external Ca^{2+}. (C) Representative traces at holding potential −60 mV showing CaCC currents with a free intracellular Ca^{2+} 0 nM under condition of application of Tg in the bath media followed by the addition of 2 mM external Ca^{2+}. (D) Representative trace showing cells pretreated with 50 μM SKF96365 that significantly inhibited currents induced by Tg with 2 mM external Ca^{2+} in HSG cells. Average IV curves (developed from maximum currents) and current density under these conditions are shown in (E), (F). *indicates values (representing mean ± SE) that are significantly different from control (*$P < 0.05$, **$P < 0.01$). (G) (H), Representative traces showing CaCC currents (with 0 nM intracellular Ca^{2+}) under conditions of bath application of 50 μM CCh with or without external Ca^{2+}. Average IV curves (developed from maximum currents) and current density under these conditions are shown in (I), (J). *indicates values (representing mean ± SE) that are significantly different from control (*$P < 0.05$, **$P < 0.01$). (K) HSG cells loaded with the chloride-sensitive dye SPQ, and stimulated with 2 μM Tg with 2 mM external Ca^{2+}. The Cl^- efflux was significant decreased by application of either 100 μM NFA, or 50 μM SKF96365. Average (30–50 cells) change in F_0/F under these conditions is shown in (L). *indicates values (representing mean ± SE) that are significantly different from control (*$P < 0.05$). (M), Representative blots indicating total and surface expression of TMEM16a in conditions of control or Tg (2 μM) stimulation for 5 min with and without external Ca^{2+}. β-actin and TFR were used as appropriate controls.

(Fig. 2A,E,F). However, when Ca^{2+} was present in the external solution (2 mM $[Ca^{2+}]_{out}$), application of Tg, showed a gradual initiation of the Cl^- currents in salivary cells (Fig. 2B, E, F) similar to observations in Figure 1. To further establish that indeed Ca^{2+} entry is essential for the activation of the Cl^- currents, simultaneous measurement of the Cl^- currents (both with and without Ca^{2+}) was performed. Addition of Tg in the absence of external Ca^{2+} showed only a transient increase in Cl^- currents; which was potentiated by the addition of external Ca^{2+} and removal of external Ca^{2+} again inhibited Cl^- currents (Fig. 2C). These results suggest that indeed Ca^{2+} entry across the plasma membrane is essential for the optimal activation of TMEM16a currents. Since store-depletion is known to increase Ca^{2+} influx across the plasma membrane through the store-operated mechanism, we further tested activation of TMEM16a currents by using SKF-96365, which is widely used to block store-operated Ca^{2+} entry channels. Importantly, cells treated with SKF-96365, showed a dramatic suppression of the Cl^- currents (Fig. 2D–F), further suggesting that Ca^{2+} influx was essential for the activation of TMEM16a currents.

Besides Tg, store-depletion can also be induced by the activation of muscarinic receptors that generate second messenger IP_3, which again leads to store depletion followed by Ca^{2+} influx. Notably, stimulation of cells with the muscarinic agonist carbachol (CCh, 50 μM) also induced the Cl^- current in presence of external Ca^{2+}, but failed to induce the Cl^- current when external Ca^{2+} concentration was decreased to 0 mM (Fig. 2G–J). Consistent with these results, store depletion (addition of Tg in the presence of external Ca^{2+}), caused a loss of intracellular Cl^- content in HSG cells (Fig. 2K, L), which was significantly decreased by the application of NFA (Fig. 2K,M). Prominently, application of SKF-96365 also inhibited the loss of intracellular Cl^- (Fig. 2K,L), suggesting Ca^{2+} influx is essential for the activation of TMEM16a. We next evaluated if the increase in TMEM16a currents is due to the activation of the channel per se or due to other mechanism(s) as Ca^{2+} has also been shown to modulate the insertion of various proteins to the plasma membrane (Pani et al., 2013). Importantly, an increase in surface expression of TMEM16a was observed in Tg-treated cells with no change in the total TMEM16a levels (Fig. 2M). Remarkably, removal of external Ca^{2+} decreased Tg-mediated increase in surface TMEM16a levels (Fig. 2M). Together, these results suggest that in HSG cells, Ca^{2+} influx via the store-operated Ca^{2+} entry channels could contribute to the regulation of Cl^- currents.

Chloride currents are inhibited by TRPC1 silencing in HSG cells

Data presented thus far suggests Ca^{2+} entry via the store-operated mechanism is essential for the activation of CaCC; however, the molecular identity of the Ca^{2+} influx channel is not known. Our previous studies have identified TRPC1 is important for store-operated Ca^{2+} entry in HSG cells (Liu et al., 2000, 2003). Application of Tg is shown to deplete intracellular ER Ca^{2+} stores, thereby activating TRPC1 or Orai1 currents in various cells. To establish the role of TRPC1 in the regulation of the CaCC, we silenced TRPC1 in HSG cells and evaluated CaCC activation. As shown in Figure 3A, expression of TRPC1 siRNA in HSG cells showed a decrease in TRPC1 protein levels, whereas control β-actin levels did not change. In contrast, cells transfected with the mock siRNA did not show any loss of TRPC1 or β-actin proteins. Notably, application of Tg along with external Ca^{2+}, showed an induction of the Cl^- currents in control HSG cells. In contrast, Tg failed to induce optimal Cl^- currents in cells expressing TRPC1 siRNA, indicating Ca^{2+} entry via the TRPC1 channel is essential for the complete activation of CaCC (Fig. 3B–D). Moreover, HSG cells expressing TRPC1 siRNA also significantly inhibited the loss of intracellular Cl^- (Fig. 3E,F), suggesting Ca^{2+} influx via TRPC1 is essential for the activation of CaCC. To further characterize Ca^{2+} entry via TRPC1 is important for CaCC activation, we artificially increased $[Ca^{2+}]_i$ concentration (by adding 300 nM $[Ca^{2+}]_i$ through the patch pipette along with the addition of Tg). Importantly, high intracellular Ca^{2+} restored CaCC in cells expressing TRPC1 siRNA; however, the Cl^- currents were still decreased when compared with control mock transfected cells (Fig. 3G-J). To evaluate the possible contribution of other TRPC channels in the regulation of CaCC, we also silenced TRPC3 in HSG cells. As shown in Figure 3K, although expression of TRPC3 siRNA in HSG cells showed a significant decrease in TRPC3 (without altering β-actin) levels, it showed no significant decrease in the activity of CaCC (Fig. 3L,M). Together these results indicate that the Cl^- current is driven by $[Ca^{2+}]_i$ and TRPC1 is an important regulator that mediates $[Ca^{2+}]_i$ concentration necessary for the complete activation of CaCC in HSG cells.

Chloride currents are observed in mouse salivary gland cells

To further confirm the molecular nature of CaCC, we next investigated the properties of the Cl^- channel in primary cells obtained from mouse salivary glands. Figure 4, illustrates an outward Cl^- current observed in mouse SMG cells, which was similar to the CaCC currents observed in HSG cells

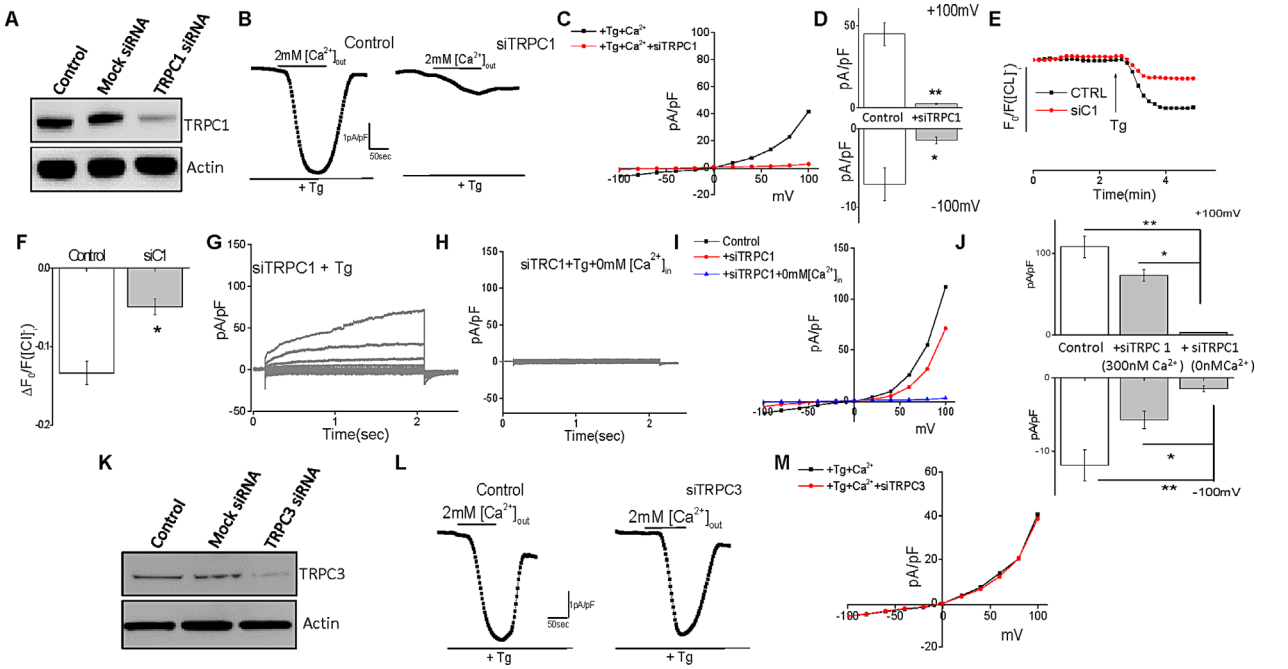

Fig. 3. CaCC currents are inhibited by TRPC1 silencing in HSG cells: (A) Representative blots indicating HSG cells expressing siRNA targeting TRPC1 or control non-targeting siRNA (Mock siRNA). β-actin was used as a loading control. (B), Representative trace (at holding potential −60 mV) showing CaCC currents (with 0 nM free intracellular Ca^{2+}) under condition of bath application of 2 μM Tg and 2 mM external Ca^{2+} from control and TRPC1 knock-down cells. Average IV curves (developed from maximum currents) and current density (8–10 recordings) under these conditions are shown in (C), (D). *indicates values (representing mean ± SE) that are significantly different from control (*$P < 0.05$, **$P < 0.01$). (E) HSG cells loaded with the chloride-sensitive dye SPQ, and stimulated with 2 μM Tg with 2 mM external Ca^{2+}. The Cl^- efflux was significantly decreased upon knock-down of TRPC1. Average (30–50 cells) changes in F_0/F under these conditions is shown in and (F). *indicates values (representing mean ± SE) that are significantly different from control (*$P < 0.05$). (G,H) Representative traces showing CaCC currents in conditions of bath application Tg with or without 300 nM free intracellular Ca^{2+} in TRPC1 knock-down cells. Average IV curves (developed from maximum currents) and current density under these conditions are shown in (I), (J). *indicates values (representing mean ± SE) that are significantly different from control (*$P < 0.05$, **$P < 0.01$). (K) Representative blots indicating HSG cells expressing siRNA targeting TRPC3 or control non-targeting siRNA. β-actin was used as loading control. (L) Representative trace showing CaCC currents under condition of bath application of 2 μM Tg and 2 mM external Ca^{2+} from control and TRPC3 knock-down cells. Average IV curves (developed from maximum currents) under these conditions are shown in (M).

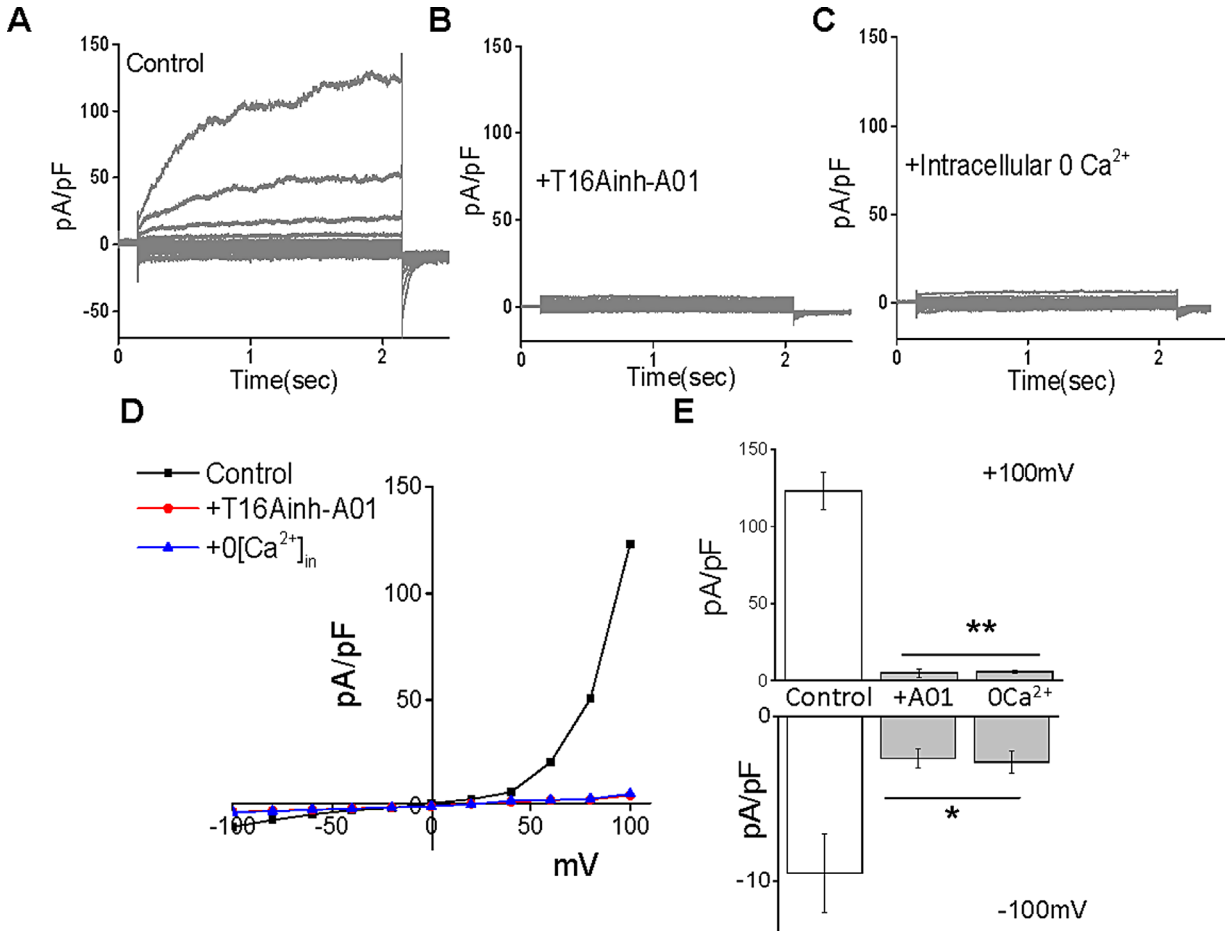

Fig. 4. CaCC currents are observed in mouse SMG cells: (A) Representative trace showing an outward current that was prompted using a voltage step protocol in conditions of 300 nM free intracellular Ca^{2+} from mouse SMG cells. (B), Bath application of 10 μM T16Ainh-A01 blocked CaCC current. The current with a free intracellular Ca^{2+} 0 nM is shown in (C). Average IV curves (developed from maximum currents) and current density under these conditions are shown in (D), (E). *indicates values (representing mean ± SE) that are significantly different from control ($^{*}P < 0.05$, $^{**}P < 0.01$).

(Fig. 1). Acinar cells obtained from mouse submandibular glands showed an outward Cl^- current, de-activating tail current upon repolarization, and strong outward rectification (Fig. 4A,D,E) upon increasing $[Ca^{2+}]_i$. Importantly, addition of T16Ainh-A01, a specific TMEM16a inhibitor, effectively abolished the Cl^- currents in SMG cells (Fig. 4B,D,E). Moreover, the Cl^- currents were totally blocked under conditions where the free intracellular Ca^{2+} was artificially decreased to 0 nM, indicating that activation of the Cl^- current in salivary gland cells is also Ca^{2+} dependent (Fig. 4C, D,E). Addition of SKF-96365, a non-specific Ca^{2+} entry blocker, also decreased the Cl^- currents (data not shown). Collectively, the close resemblance of CaCC properties presented in Figure 4, suggests that the endogenous CaCC currents in mouse SMG cells is generated by TMEM16a. These results are consistent with a previous study indicating that TMEM16a encodes the CaCC channel in salivary gland cells (Romanenko et al., 2010).

Salivary gland cells obtained from TRPC1 knockout mice showed an inhibition in the chloride currents

To further test the hypothesis that TRPC1 regulates CaCC activity, we next used mice lacking TRPC1 to determine whether TRPC1 is critical for the regulation of CaCC currents in primary acinar cells. Expression of TRPC1 was absent in $TRPC1^{-/-}$ mice, in contrast, no change in TMEM16a expression was observed between wild type and $TRPC1^{-/-}$ mice (Fig. 5A). Importantly, the whole-cell CaCC currents recorded using voltage clamp steps in acinar cells isolated from submandibular glands were activated by varying intracellular Ca^{2+}. Application of Tg along with the addition of 2 mM external Ca^{2+} showed induction of the CaCC currents in SMG cells obtained from wild-type mice. Whereas, SMG cells isolated from $TRPC1^{-/-}$, failed to show optimal activation of the CaCC currents under similar conditions (Fig. 5B–D). To further evaluate the role of intracellular Ca^{2+} we artificially increased intracellular Ca^{2+} via the patch pipette in SMGs obtained from $TRPC1^{-/-}$ mice. Notably, high intracellular Ca^{2+} (300 nM) significantly increased the CaCC currents in $TRPC1^{-/-}$ mice (Fig. 5E–G) and as the expression of TMEM16a in wild type and $TRPC1^{-/-}$ mice was similar, it could be suggested that the loss of Cl^- currents in $TRPC1^{-/-}$ mice is not due to changes in the expression of TMEM16a, but due to the loss of elevated cytosolic Ca^{2+} levels (due to loss of TRPC1). Together, these results are consistent with TRPC1 being the major Ca^{2+} channel that regulate TMEM16a currents, which could drive salivary fluid secretion.

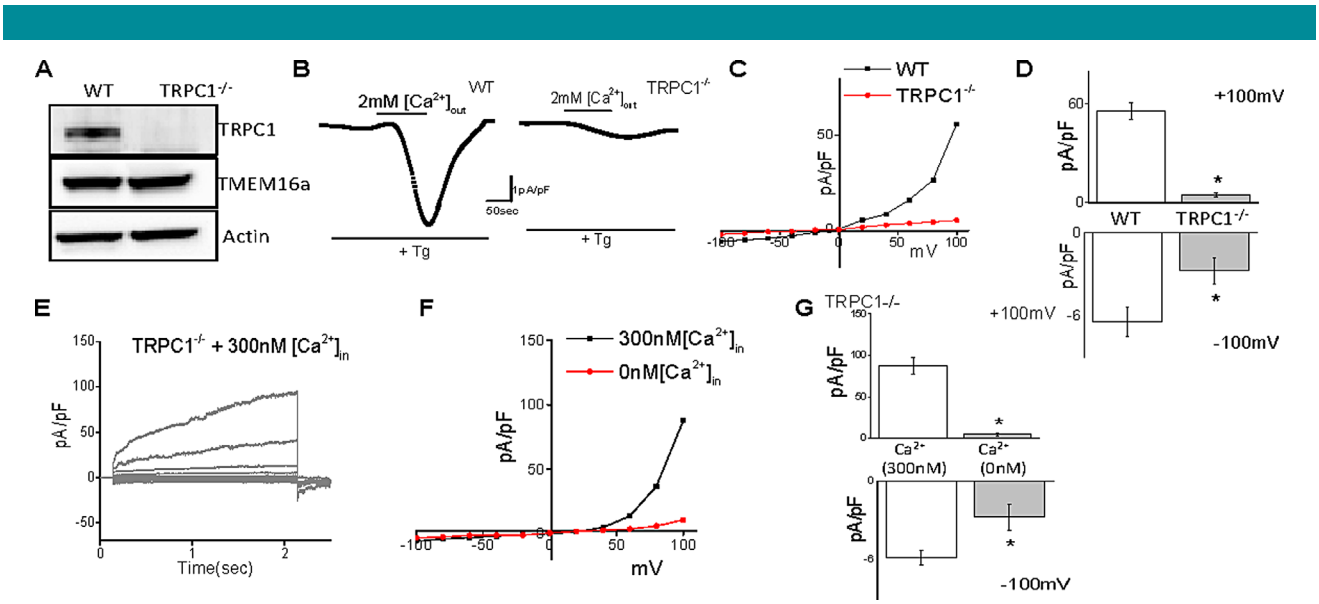

Fig. 5. CaCC currents are inhibited by the loss of TRPC1 in mouse SMG cells: (A) Representative blots indicating mouse SMG cells expressing TRPC1 and TMEM16a from wild type or TRPC1 knockout mice. β-actin was used as a loading control. (B) Representative trace showing CaCC currents (with free intracellular Ca^{2+} 0 nM) under condition of bath application 2 μM Tg followed by the addition of 2 mM external Ca^{2+} from control and TRPC1 knockout acinar cells at holding potential −60 mV. Average IV curves (developed from maximum currents) and current density under these conditions are shown in (C), (D). *indicates values (representing mean ± SE) that are significantly different from control ($P < 0.05$). (E) Representative trace showing CaCC currents in conditions of 300 nM free intracellular Ca^{2+} from TRPC1 knockout cells. Average IV curves (developed from maximum currents) at 300 nM or 0 nM free intracellular Ca^{2+} in TRPC1 knockout cells are shown in (F). Average (8–10 recordings) current density at +100 mV and −100 mV under these conditions is shown in (G). *indicates values (representing mean ± SE) that are significantly different from control ($P < 0.05$).

Discussion

TMEM16a channels are widely expressed in exocrine cells including salivary gland tissues (Caputo et al., 2008). The Cl^- currents characterized in this study exhibited a marked outward rectification, which were abolished upon the application of NFA in both HSG cells and in primary acinar cells isolated from mouse submandibular glands. More importantly, the Cl^- currents were blocked by T16Ainh-A01, which is a specific antagonist for TMEM16a channel and the biophysical properties of the Cl^- channel observed in salivary gland cells were essentially similar to that of the native TMEM16a channels (Ferrera et al., 2010; Huang et al., 2012). Previous studies have shown that the expression of TMEM16a is sufficient to produce a Cl^- current, which shares most of the properties of endogenous CaCC (Ferrera et al., 2010; Pedemonte and Galietta, 2014). The presence of TMEM16a protein further consolidates the existence of CaCC in salivary gland cells and an addition of a CFTR inhibitor failed to inhibit CaCC, further suggesting TMEM16a is the major Cl^- efflux channel in salivary cells. Overall, the data presented here shows a direct link between TMEM16a channel and CaCC currents and suggests TMEM16a encodes CaCC in both HSG cell line and native salivary gland cells that is activated by increase in intracellular Ca^{2+} levels.

Ca^{2+} signaling regulates saliva secretion

Salivary gland fluid secretion is regulated by the activation of Ca^{2+} signaling machinery (Ambudkar, 2012). Increase in $[Ca^{2+}]_i$ at specific regions of the cells is the main determinant for sustained fluid and electrolyte secretion in salivary gland acinar cells as it could regulate several major ion flux mechanisms as well as the water channel that are required for saliva secretion (Pani et al., 2013; Pang et al., 2014). Na^+/H^+ exchanger, Ca^{2+}-activated K^+ channels, Na^+ K^+ Cl^- cotransporter, CaCC, and AQP5 all contribute to a varying extent towards fluid secretion as seen by the impact of their deletion on saliva flow and its ionic composition (Melvin et al., 2005; Roussa, 2011). A wealth of data suggests that an increase in $[Ca^{2+}]_i$ is paralleled by an increase in Cl^- influx (Ambudkar, 2012), but the mechanism as how $[Ca^{2+}]_i$ regulates saliva secretion is not completely understood. Regulation of chloride channels, and consequently saliva secretion, depends on a sustained increase in $[Ca^{2+}]_i$. Furthermore, it has now been shown that Ca^{2+} entry in acinar cells is activated in response to agonist-stimulated PIP_2 hydrolysis that generates second messenger IP_3, which binds to IP_3R in the ER in order to initiate Ca^{2+} signaling. Consistent with this, IP_3R2 and IP_3R3 knockout mice showed agonist-mediated loss of internal Ca^{2+} release as well as Ca^{2+} entry in acinar cells and displayed significant attenuation of neurotransmitter-stimulated fluid secretion (Futatsugi et al., 2005; Ambudkar, 2012). SOCE is an important Ca^{2+} entry mechanism which is activated by the generation of second messengers such as IP_3 (Ambudkar, 2012; Pang et al., 2014) and could regulate various transporters and ion channels essential for saliva secretion.

TRPC1 augment CaCC current activation

Studies using human submandibular gland cell line first demonstrated that TRPC1 contributes towards store-operated Ca^{2+} entry (Liu et al., 2001, 2003; Caputo et al., 2008; Cho et al., 2014). Generation of mice lacking TRPC1 further provide evidence for the role of TRPC1 in salivary acinar cells (Liu et al., 2007). Importantly, these mice displayed a decrease in Ca^{2+} entry as well as fluid secretion; however, the mechanism as why saliva secretion was decreased is not well known. In addition, a recent study also showed that TRPC1 contributes to SOCE in pancreatic acinar cells where it has a

role in the modulation of Ca^{2+}-activated Cl^- currents (Ambudkar, 2012). The kinetics of Cl^- release seem to reflect the kinetics of $[Ca^{2+}]_i$ transients, suggesting a direct mechanistic coupling between the two ions (Romanenko et al., 2010; Pang et al., 2014). The data presented here also showed that the amplitude of CaCC was markedly decreased in TRPC1, but not in TRPC3, knock-down cells. Non-specific TRPC channels inhibitor, SKF-96365 also decreased CaCC currents in HSG cells. In contrast, store depletion activated TRPC1-mediated Ca^{2+} entry significantly facilitated CaCC currents especially in the presence of external Ca^{2+}, suggesting TRPC1-mediated Ca^{2+} entry is needed for the activation of CaCC currents. Although our data suggests the role of Ca^{2+} influx via the TRPC1 channels, we cannot completely rule the possibility for the role of ER Ca^{2+} in modulating CaCC currents as the electrophysiological methods used were specific for the maximal activation of TRPC1 channels. One important aspect of our study was the observation that application of Tg in the absence of external Ca^{2+} did not increased TMEM16a surface expression. This indicates a novel mechanism of Ca^{2+} influx via the TRPC1 channels could modulate CaCC currents by facilitating the membrane insertion of TMEM16a channels. However, as basal insertion of CaCC channels was not altered, this could be an added mechanism needed for the activation of CaCC channels and would be interesting to see if similar mechanism is also present in other secretory cells. Nonetheless, this could be a novel mechanism and explains as how TRPC1-induced Ca^{2+} entry could modulate TMEM16a function and more research is needed to fully establish this phenomenon.

Consistent with the observations in HSG cell lines, we also found similar results in native submandibular acinar cells. Stimulation or inhibition of TRPC1 channel had a reciprocal effect on CaCC activity in native submandibular acinar cells. Moreover, submandibular acinar cells isolated from TRPC1 knockout mice displayed a significant decrease in CaCC currents and the effect of Tg-mediated increase in Cl^- currents was abolished in cells expressing TRPC1 siRNA. Importantly, artificially increasing intracellular Ca^{2+} restored the CaCC currents in cells expressing TRPC1 siRNA or cells obtained from TRPC1 knock-out mice. However, when compared with control cells, CaCC currents were still lower, suggesting that TRPC1 might have additional role in modulating CaCC currents besides just increasing intracellular Ca^{2+}. Taken together, these results clearly demonstrate a close interaction between TRPC1 and CaCC channels in salivary gland cells. Interestingly, functional interplay between TRPC1–TMEM16a is not only restricted to Ca^{2+} entry, as anion selectivity of TMEM16a is also shown to be dynamically regulated by the Ca^{2+}/calmodulin complex. Studies revealed that the direct association between TMEM16a and calmodulin at high $[Ca^{2+}]_i$ is responsible for changes in anion permeability (Jung et al., 2013). Ca^{2+}/calmodulin has also been shown to be tightly associated with STIM1/TRPC1 complex (Galan et al., 2011) and TRPC1 has been shown to be activated via STIM1 and its channel activity is modulated by calmodulin (Singh et al., 2002), which could also modulate TMEM16a currents in salivary gland cells.

Conclusions

We previously reported that loss of TRPC1 inhibits saliva secretion, but the mechanism was not well understood. The purpose of this study was to establish if store-operated Ca^{2+} entry regulates TMEM16a currents in salivary cells. Major findings of the present study are that TMEM16a channel is crucial for Cl^- efflux and that TRPC1 is a critical regulator for TMEM16a channel function in salivary gland cells. TRPC1 provides the sustained Ca^{2+} entry (upon store depletion) that is essential for complete activation of TMEM16a to modulate Cl^- efflux. TRPC1 function also increased the surface expression of TMEM16a and loss of TRPC1 function inhibited TMEM16a activation, which could be the mechanism as how TRPC1 modulates saliva secretion. The data presented here provides genetic evidence for the physiological function for TRPC1 in the regulation of TMEM16a in salivary gland cells. We suggest that TRPC1 could be a potentially useful target molecule for the activation of ion channels and transporters that modulate fluid secretion and thus could aid in the treatment of salivary gland dysfunctions.

Author Contributions

B.S. designed and supervised the experiments; Y.S. performed all the experiments; LB provided the TRPC1 knock-out mice and all authors analyzed the data and critically reviewed and approved the final version. All experiments were carried out at the University of North Dakota.

Funding

Financial support was received from the National Institutes of Health (DE017102) awarded to B.B.S and the Intramural Research Program of the NIH (project Z01-ES-101684) to L.B.

Literature Cited:

Ambudkar IS. 2012. Polarization of calcium signaling and fluid secretion in salivary gland cells. Curr Med Chem 19:5774–5781.
Caputo A, Caci E, Ferrera L, Pedemonte N, Barsanti C, Sondo E, Pfeffer U, Ravazzolo R, Zegarra-Moran O, Galietta LJ. 2008. TMEM16A, a membrane protein associated with calcium-dependent chloride channel activity. Science 322:590–594.
Catalan MA, Kondo Y, Pena-Munzenmayer G, Jaramillo Y, Liu F, Choi S, Crandall E, Borok Z, Flodby P, Shull GE, Melvin JE. 2015. A fluid secretion pathway unmasked by acinar-specific Tmem16A gene ablation in the adult mouse salivary gland. Proc Natl Acad Sci USA 112:2263–2268.
Cho HJ, Park SM, Kim IK, Nam IK, Baek KE, Im MJ, Yoo JM, Park SH, Ryu KJ, Han HT, Kim HJ, Hong SC, Kim KD, Pak Y, Kim JW, Lee CW, Yoo J. 2014. RhoGDI2 promotes epithelial-mesenchymal transition via induction of Snail in gastric cancer cells. Oncotarget 5:1554–1564.
Davis AJ, Shi J, Pritchard HA, Chadha PS, Leblanc N, Vasilikostas G, Yao Z, Verkman AS, Albert AP, Greenwood IA. 2013. Potent vasorelaxant activity of the TMEM16A inhibitor T16A(inh) - A01. Br J Pharmacol 168:773–784.
Ferrera L, Caputo A, Galietta LJ. 2010. TMEM16A protein: A new identity for Ca(2+)-dependent Cl(−) channels. Physiology 25:357–363.
Ferrera L, Zegarra-Moran O, Galietta LJ. 2011. Ca2+-activated Cl-channels. Compre Physiol 1:2155–2174.
Frizzell RA, Hanrahan JW. 2012. Physiology of epithelial chloride and fluid secretion. Cold Spring Harb Perspect Med 2:a009563.
Futatsugi A, Nakamura T, Yamada MK, Ebisui E, Nakamura K, Uchida K, Kitaguchi T, Takahashi-Iwanaga H, Noda T, Aruga J, Mikoshiba K. 2005. IP3 receptor types 2 and 3 mediate exocrine secretion underlying energy metabolism. Science 309,2232–2234.
Galan C, Dionisio N, Smani T, Salido GM, Rosado JA. 2011. The cytoskeleton plays a modulatory role in the association between STIM1 and the Ca2+ channel subunits Orai1 and TRPC1. Biochem Pharmacol 82:400–410.
Hartzell C, Putzier I, Arreola J. 2005. Calcium-activated chloride channels. Annu Rev Physiol 67:719–758.
Huang F, Rock JR, Harfe BD, Cheng T, Huang X, Jan YN, Jan LY. 2009. Studies on expression and function of the TMEM16A calcium-activated chloride channel. Proc Natl Acad Sci USA 106:21413–21418.
Huang F, Wong X, Jan LY. 2012. International union of basic and clinical pharmacology. LXXXV: Calcium-activated chloride channels. Pharmacol Rev 64:1–15.
Jung J, Nam JH, Park HW, Oh U, Yoon JH, Lee MG. 2013. Dynamic modulation of ANO1/TMEM16A HCO3(−) permeability by Ca2+/calmodulin. Proc Natl Acad Sci USA 110:360–365.
Lee RJ, Foskett JK. 2010. Mechanisms of Ca2+-stimulated fluid secretion by porcine bronchial submucosal gland serous acinar cells. Am J Physiol Lung Cell Mol Physiol 298: L210–231.
Liu X, Cheng KT, Bandyopadhyay BC, Pani B, Dietrich A, Paria BC, Swaim WD, Beech D, Yildrim E, Singh BB, Birnbaumer L, Ambudkar IS. 2007. Attenuation of store-operated Ca2+ current impairs salivary gland fluid secretion in TRPC1(-/-) mice. Proc Natl Acad Sci USA 104:17542–17547.
Liu X, Ong HL, Pani B, Johnson K, Swaim WB, Singh B, Ambudkar I. 2010. Effect of cell swelling on ER/PM junctional interactions and channel assembly involved in SOCE. Cell Calcium 47:491–499.
Liu X, Singh BB, Ambudkar IS. 2003. TRPC1 is required for functional store-operated Ca2+ channels. Role of acidic amino acid residues in the S5-S6 region. J Biol Chem 278:11337–11343.
Liu X, Wang W, Singh BB, Lockwich T, Jadlowiec J, O'Connell B, Wellner R, Zhu MX, Ambudkar IS. 2000. Trp1, a candidate protein for the store-operated Ca(2+) influx mechanism in salivary gland cells. J Biol Chem 275:3403–3411.
Melvin JE, Yule D, Shuttleworth T, Begenisich T. 2005. Regulation of fluid and electrolyte secretion in salivary gland acinar cells. Annu Rev Physiol 67:445–469.
Ong HL, Cheng KT, Liu X, Bandyopadhyay BC, Paria BC, Soboloff J, Pani B, Gwack Y, Srikanth S, Singh BB, Gill DL, Ambudkar IS. 2007. Dynamic assembly of TRPC1-STIM1-Orai1 ternary complex is involved in store-operated calcium influx.

Evidence for similarities in store-operated and calcium release-activated calcium channel components. J Biol Chem 282:9105–9116.
Ousingsawat J, Martins JR, Schreiber R, Rock JR, Harfe BD, Kunzelmann K. 2009. Loss of TMEM16A causes a defect in epithelial Ca2+-dependent chloride transport. J Biol Chem 284:28698–28703.
Pang C, Yuan H, Ren S, Chen Y, An H, Zhan Y. 2014. TMEM16A/B associated CaCC: Structural and functional insights. Protein Pept Lett 21:94–99.
Pani B, Liu X, Bollimuntha S, Cheng KT, Niesman IR, Zheng C, Achen VR, Patel HH, Ambudkar IS, Singh BB. 2013. Impairment of TRPC1-STIM1 channel assembly and AQP5 translocation compromise agonist-stimulated fluid secretion in mice lacking caveolin1. J Cell Sci 126:667–675.
Pedemonte N, Galietta LJ. 2014. Structure and function of TMEM16 proteins (anoctamins). Physiol Rev 94:419–459.
Romanenko VG, Catalan MA, Brown DA, Putzier I, Hartzell HC, Marmorstein AD, Gonzalez-Begne M, Rock JR, Harfe BD, Melvin JE. 2010. Tmem16A encodes the Ca2+-activated Cl- channel in mouse submandibular salivary gland acinar cells. J Biol Chem 285:12990–13001.
Roussa E. 2011. Channels and transporters in salivary glands. Cell Tissue Res 343:263–287.
Schroeder BC, Cheng T, Jan YN, Jan LY. 2008. Expression cloning of TMEM16A as a calcium-activated chloride channel subunit. Cell 134:1019–1029.
Singh BB, Liu X, Tang J, Zhu MX, Ambudkar IS. 2002. Calmodulin regulates Ca^{2+}-dependent feedback inhibition of store-operated Ca^{2+} influx by interaction with a site in the C-terminus of TRPC1. Mol Cell 9:739–750.
Sun Y, Sukumaran P, Varma A, Derry S, Sahmoun AE, Singh BB. 2014. Cholesterol-induced activation of TRPM7 regulates cell proliferation, migration, and viability of human prostate cells. Biochim Biophys Acta 1843:1839–1850.
Takayama Y, Shibasaki K, Suzuki Y, Yamanaka A, Tominaga M. 2014. Modulation of water efflux through functional interaction between TRPV4 and TMEM16A/anoctamin 1. Faseb J 28:2238–2248.
Thomas-Gatewood C, Neeb ZP, Bulley S, Adebiyi A, Bannister JP, Leo MD, Jaggar JH. 2011. TMEM16A channels generate Ca(2)(+)-activated Cl(−) currents in cerebral artery smooth muscle cells. Am J Physiol Heart Circ Physiol 301:H1819–1827.
Viitanen TM, Sukumaran P, Lof C, Tornquist K. 2013. Functional coupling of TRPC2 cation channels and the calcium-activated anion channels in rat thyroid cells: Implications for iodide homeostasis. J Cell Physiol 228:814–823.
Yang YD, Cho H, Koo JY, Tak MH, Cho Y, Shim WS, Park SP, Lee J, Lee B, Kim BM, Raouf R, Shin YK, Oh U. 2008. TMEM16A confers receptor-activated calcium-dependent chloride conductance. Nature 455:1210–1215.

Supporting Information

Additional supporting information may be found in the online version of this article at the publisher's web-site.